Customization of Digital Circuit for Material-Independent Eddy Current Proximity Sensor for Active Magnetic Bearings

Rafal P. Jastrzebski[1,a], Kimmo Tolsa[1,b], Matti Iskanius[1,c]

[1]Dept. of Electrical Engineering, LUT Energy, Lappeenranta University of Technology,
PO 20, 53851 Lappeenranta, Finland
[a]rafal.jastrzebski@lut.fi, [b]kimmo.tolsa@lut.fi, [c]matti.iskanius@lut.fi

Abstract: The state of the art, commercial eddy current sensors can provide excellent quality of the measured position; however, the easier system integration, size of the conditioning electronics, cost, and interfacing delays are unfavorable. In this paper, a customization of the basic conventional single-coil eddy current proximity sensor for active magnetic bearings is presented. The signal conditioning is designed to be integrated with the main signal processing unit, which can also incorporate the active magnetic bearing system controller. The nonlinearities and dependencies on the electromagnetic properties of the target material are eliminated using software implementation. The highest signal to noise ration is observed for the aluminium-alloy target. It is shown that for the studied sensor the measuring range and accuracy are limited when under the material-independent operation.

Keywords: Eddy Current Sensor, Air-gap Detection, Measured Material Properties, Field Programmable Gate Arrays

Introduction

The reliable and high-performance control of an active magnetic bearing (AMB) rotor system depends on the quality of the measurements. Direct position measurement using an eddy-current sensor is widely used for air-gap detection because of the small size, sensitivity, anti-noise, and dynamic performance [1]. The available state-of-the-art commercial sensors provide some excellent properties, for example, very high resolution, but from the perspective of the AMB system, they have disadvantages such as the large size of electronics for signal conditioning, the need for manual calibration that cannot be carried out using the same user interface as the one for the controller, operation with specific target materials, and a high cost. Moreover, a delay is introduced by the system integration interface and sampling of an analog output.

The literature presents different methods to customize and improve proximity sensors, which are based on the eddy current principles. Examples include using many excitation coils with a single search coil, applying multi-frequency excitation [2], and adding a compensation coil for the temperature compensation [3]. Yu and Du [4,5] studied how to eliminate the effect of material properties on the output of the eddy current sensors. In [5], it is presented that the impedances of the active coil for different target materials are equivalent when projected to the one particular plane. Dong et al. [6] introduced an analog implementation of the electronics of a material-independent sensor. However, the comparison between the properties of the material-dependent sensor and the material-independent one were missing.

The described work discusses the customization of the eddy-current proximity sensors to exactly meet the needs of an individual AMB system with regard to certain application characteristics at a lower cost than the one of off-the-shelf sensors. The paper extends the

ideas introduced in [4,5] and [6] by introducing a digital implementation of the circuit for a material-independent sensor. This results in better nonlinearity compensation (compared with [6]) and improved system integration. The operation of the eddy current sensor when intended for the particular different target materials is compared with the material-independent configuration. The digital signal processing implemented in the field programmable gate array (FPGA) allows a seamless integration with the similarly implemented plant controllers [7]. This reduces the cost and size of the overall control cabinet. The configuration and scaling of the sensors can be integrated into the user interface of the AMB control unit.

Measurement principles and material-independent operation

For the basic conventional sensor, the same coil can be utilized for the excitation and for the sensing. A high-frequency alternating current runs through the coil producing a high-frequency magnetic field. Because of the energy dissipation, the amplitudes and phases of the oscillating current and the voltage signals in the coil vary according to the distance of the target to be measured. Hence, the variations of the air-gap between the coil and the target produce the changes in the impedance of the transducer coil. We define the equivalent impedance as the total coil voltage, which is the sum of the coil self-induced voltage and the eddy current's induced voltage, divided by the coil current.

The equivalent-valued method presented in [5,6] assumes that the change of the measured impedance for different target metals and for the same measurement distance is approximately linear (Fig.1). If the linear functions of the measured impedances Z of different targets considered for different distances are parallel, their offset values (intersections between the dotted lines and the X axis in Fig. 1) can be determined. These offsets are referred to as equivalent projection impedances Z_{pi} and can be computed using the angle of the projection plane θ and the angle of the impedance φ such as

$$Z_p = Z\cos(\theta-\varphi),\ Z_p = Z\cos(\theta-\pi/2),\ Z_{pi} = Z\frac{\cos(\theta-\varphi)}{\cos(\theta-\pi/2)}, \tag{1}$$

where the Z_p is the projection of the coil impedances onto the projecting plane, which is perpendicular to the linear functions of impedances under different measuring targets.

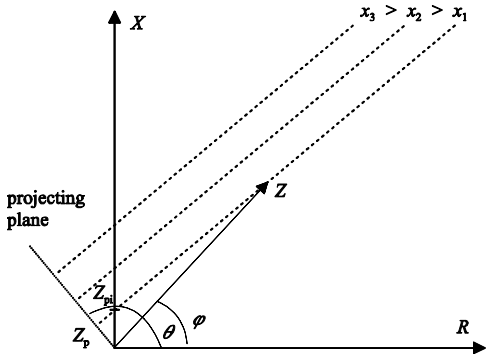

Figure 1: Projecting plane in the equivalent-valued method.

Implementation

In the sensor probe, an alternating current, with the frequency f_e=476.19 kHz, runs through the coil. The coil radius is approximately equal to 0.65 mm and the number of turns is 100. The sensor is connected to the test board, shown in Fig. 2, with the sensor cable. The test board comprises transducer amplifiers, 14-bit analog-to-digital converters (ADCs), 14-bit digital-to-analog converters (DAC), Xilinx's Spartan®-3 FPGA (xc3s1000) and an USB interface for easy communication with the PC. The sampling frequency f_s=1470.6 kHz. The N consecutive samples of the coil current and voltage signals are collected. The phase differences of the sampled signals $\boldsymbol{\chi} = [0 \quad 1 \quad \ldots \quad N-1]^{\mathrm{T}} 2\pi f_e / f_s$.

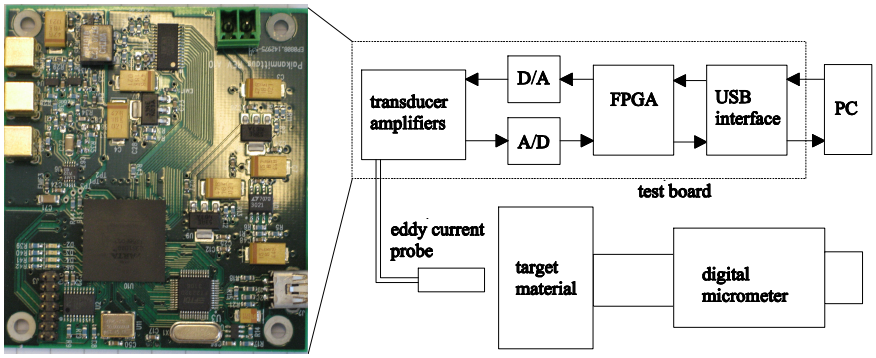

Figure 2: Test-rig for studying a material–independent proximity sensor and the test board.

Using the periodical model $\mathbf{u}(\chi)=C_u\cos(\chi)+S_u\sin(\chi)+O_u$ to express the measured values of voltage and current signals as a function of χ and applying the least squares estimate, the equivalent coil impedance for the each tested material and position is

$$\begin{bmatrix} C_u & C_i \\ S_u & S_i \\ O_u & O_i \end{bmatrix} = \left(\boldsymbol{\Phi}^{\mathrm{T}}\boldsymbol{\Phi}\right)^{-1}\boldsymbol{\Phi}^{\mathrm{T}}\left[\mathbf{u}(\chi) \quad \mathbf{i}(\chi)\right],\ Z = \frac{C_u C_i + S_u S_i + j\left(C_u S_i - S_u C_i\right)}{C_i^{\,2} S_i^{\,2}}, \tag{2}$$

where $\boldsymbol{\Phi} = [\cos(\chi) \quad \sin(\chi) \quad \mathbf{I}]$. Using N=155 for computation of the each impedance value, results in the sensor bandwidth of 2.4 kHz. For most of the AMB applications, the bandwidth is sufficient as the frequencies above 1 kHz are rarely considered.

The computation of C, S, and O coefficients requires 6 multiplications and 6 additions per sampling period. The most computationally intensive is the single division required to compute the impedance once every N samples. Additionally, the dot product of the voltage and current vectors can be utilized instead of the computationally costly impedance. For the material-independent operation, the cosine function can be easily implemented in the FPGA as a look-up table.

The system safety and reliability can be increased by applying two sensors per each axis and per each measuring plane. By default, the controller operates using two sensors for measuring the rotor displacement. In the case of the detected failure of one of the sensors, the controller can autonomously switch to use only the correctly working sensor. A simple to realize and effective method to determine the sensor error is to test if the measured current and voltage signals are in the measuring range and whether the consecutive samples have different values because of the phase difference.

Experimental evaluation

The design is evaluated by measuring the position distance with a digital micrometer, which has accuracy of 1 µm, between the active coil sensor tip and five different target materials: c1: structural steel (S355J0), c2: aluminium-alloy (AIMg5), c3: stainless steel (AISI304), c4: spring steel (SS2090), and c5: brass (Ms358 – CuZn39Pb3).

In the case of the material-dependent operation, the measured relations between resistance, reactance, dot product and the air-gap are presented in Figs. 3 and 4. For the construction of the interpolation look-up tables, the measurements are carried out in series of 20 measurements every 100 µm. For each measured displacement, the mean values of the resistance, reactance, absolute impedance, and dot product are stored in the look-up tables. Using the look-up tables and a third-order spline interpolation, the signal-to-noise ratio (SNR) of position measurements, which are based on different physical quantities, are determined. The SNR is equivalent to a resolution, which can be described as the smallest change of a quantity that can be reliably measured.

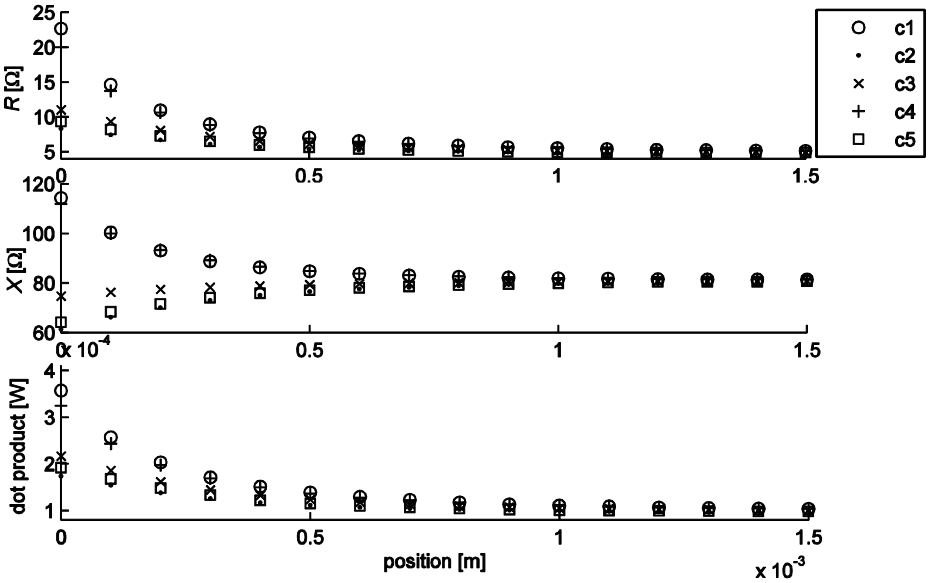

Figure 3: Measured resistance, reactance, and impedance angle for different materials.

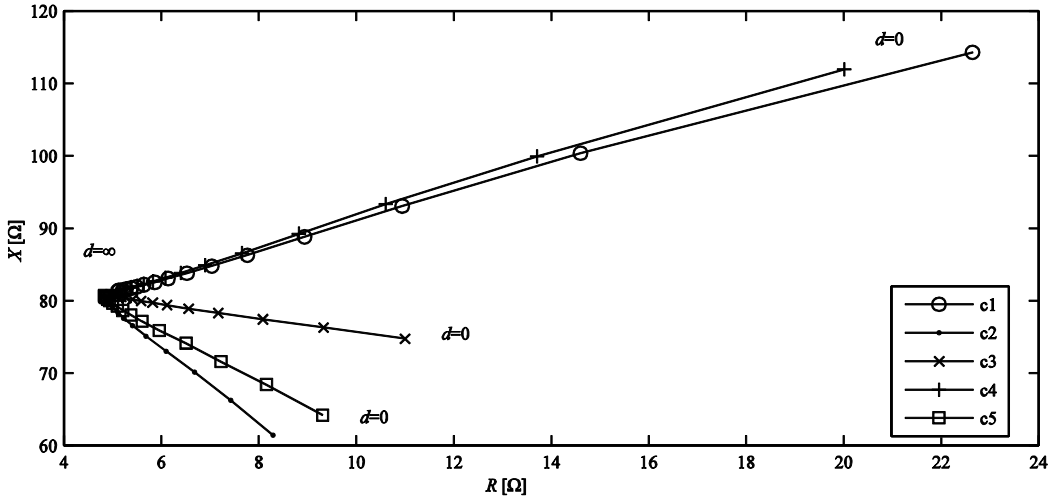

Figure 4: Measured resistance and reactance for different distances *d* and materials c1-5.

For example, for the reactance SNR= $\mu_{|X(p)-X(p=11\text{mm})|} / \sigma_{X(p)}$, where μ and σ are the mean value and the standard deviation of the quantity, respectively. For the computation of the SNR, depicted in Fig. 5, the measurements were repeated after shifting the displacements by 25 µm. An interesting compromise between the resolution and the computational burden could be achieved by using the structural steel and the dot product for measuring displacement. However, the best choice in terms of resolution is to use the aluminium alloy and the reactance-based position measurement. Aluminium is the preferred material because it counters the electrical runout errors and inhomogeneity [8] in the applications with a rotating target. The mean errors and their standard deviations when measuring a displacement based on the impedance are shown in Fig 6. We define a relative resolution of the full scale output (FSO) as the worst standard deviation of the position error registered for 20 consecutive samples divided by the measuring range. The recorded relative resolutions of the FSO of different targets for the measuring range from 0 µm to 500 µm are: c1: 0.77%, c2: 0.67% c3: 2.98%, c4: 0.62%, c5: 0.76%. The linearity is less than 1% for all targets.

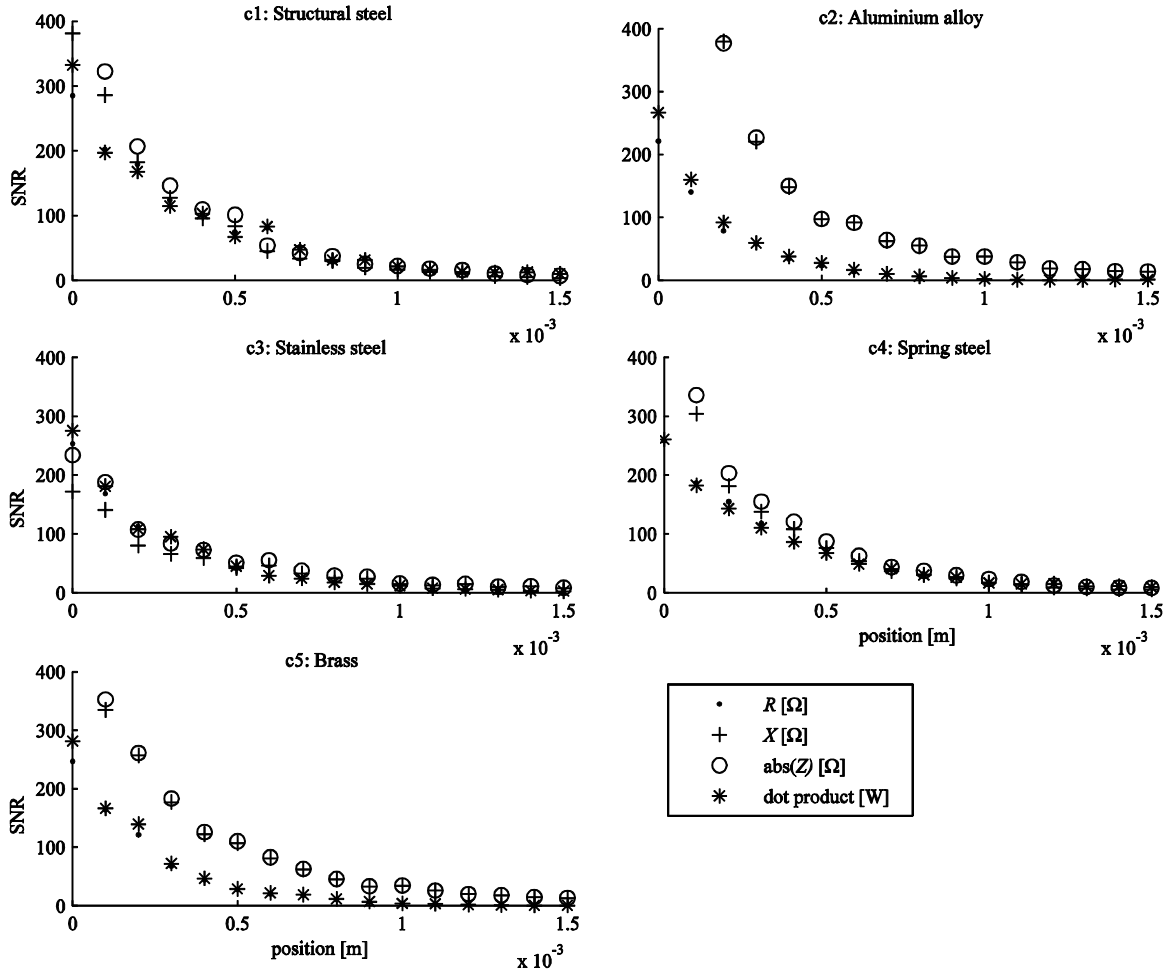

Figure 5: Measured SNR for different measured signals. SNR is expressed as a ratio of mean to standard deviation of the measured signal minus the signal value at the maximum distance 11 mm.

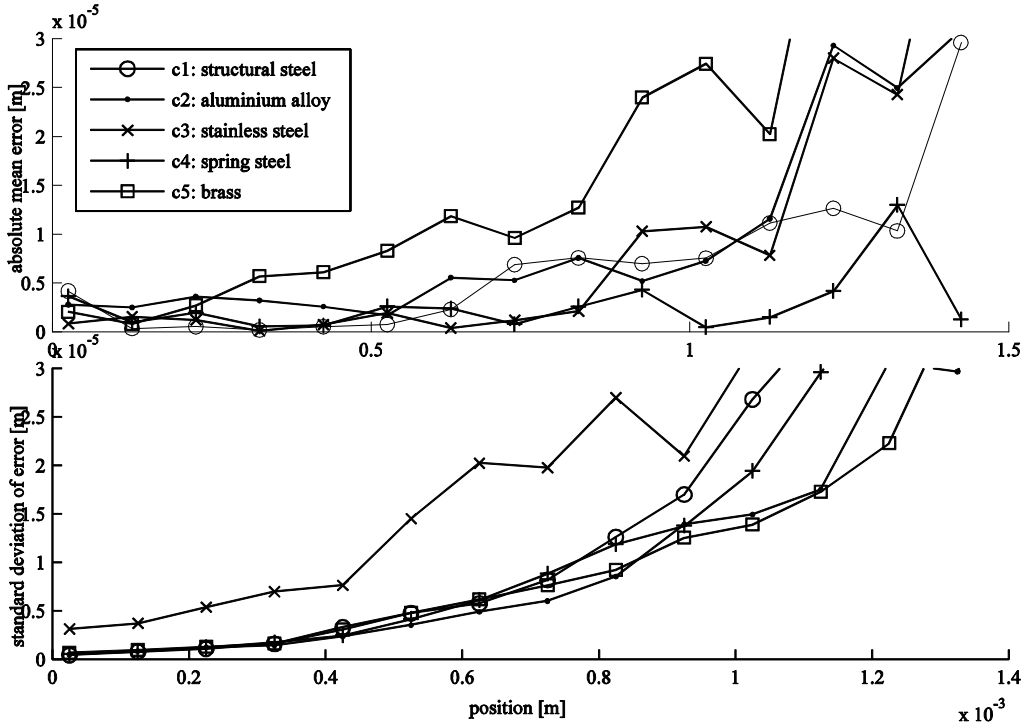

Figure 6: Mean position error and its standard deviation when measuring the absolute value of impedance for the tested materials at different distances.

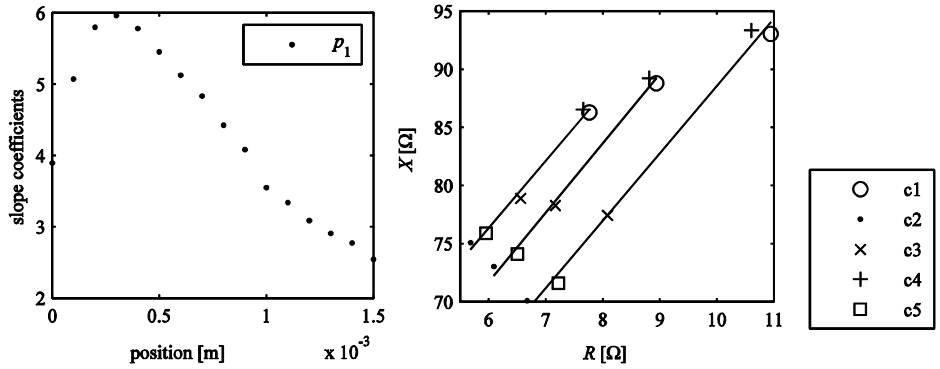

Figure 7: Tangent of the linearized impedance projections (slope coefficients) in the left and the linearized impedance projections at 100, 200, and 300 µm for materials c1-5.

In the case of the material-independent operation, as it can be seen in Fig. 7, the measuring range is limited because the linear functions of the measured impedances of different targets considered for different distances are not parallel. The tests for the five materials gave the resolution of 5.9% FSO in the measuring range from 100 to 300 µm.

Conclusions

For the best results, the eddy-current sensor should be calibrated to the same target material as in the application, preferably aluminium. Stainless steel should not be selected as a target material. The measured signal linearity can be increased by increasing the size of look-up tales used for the interpolation. The material-independent operation is only feasible in the limited measuring range.

As an outlook, the resolution and the bandwidth could be improved by increasing the sampling frequency. The more optimized multi-coil sensor and not the single coil could be applied.

References

[1] J. Boehm, R. Gerber, N.R.C. Kiley: Sensors for Magnetic Bearings, *IEEE Transactions on Magnetics*, Vol. 29, No. 6 (1993) pp. 2962–2964.

[2] T. Chady and R. Sikora: Optimization of Eddy-Current Sensor for Multifrequency Systems, *IEEE Transactions on Magnetics*, Vol. 39, No. 3 (2003), pp. 1313–1316.

[3] Q. Li, F. Ding: Novel displacement eddy current sensor with temperature compensation for electrohydraulic valves, *Sensors and Actuators*, A 122 (2005) pp. 83–87.

[4] Y.T. Yu, P.A. Du, Z.W. Wang: Study on the electromagnetic properties of eddy current sensor, In Proceedings of the IEEE International Conference on mechatronics and automation (2005), pp. 1970–1975.

[5] Y.T. Yu, P.A. Du, Research on the correlation between measured material properties and output of eddy current sensor, In Proceedings of the IEEE ICIT (2005), pp. 428–431.

[6] W. Dong, P. Du, Y. Yu, and L. Xu, Design and Implementation of Functional Measuring Circuit for Material-Independent Eddy Current Sensor, In Proceedings of the IEEE ICMA (2008), pp. 319–323.

[7] R. Jastrzebski, R. Pöllänen, O. Pyrhönen, A. Kärkkäinen, J. Sopanen: Modeling and Implementation of Active Magnetic Bearing Rotor System for FPGA-based Control, In Proceedings of the Tenth International Symposium on Magnetic Bearings, Martigny, Switzerland (2006).

[8] G.Y. Tian, Z.X. Zhao, R. W. Baines, The research of inhomogeneity in eddy current sensors, *Sensors and Actuators* A 69, pp. 148–151, 1998.